Műszaki Tudományos Közlemények vol. 21. (2024) 21–30.
DOI: Hungarian: https://doi.org/10.33895/mtk-2024.21.04
English: https://doi.org/10.33894/mtk-2024.21.04

CONSTRUCTION OF MPA ANTENNA ROTATION SYSTEM FOR INTERFERO-METRIC “IN-SITU” MEASUREMENTS

Szabolcs Sándor DIÓS,[1] Abdullah MASUK,[2] Tamás DINYA,[3] Attila SZÁNTÓ,[4] Dávid PETTENDI,[5] István BALAJTI[6]

[1] *Debrecen University, Mechatronics Department, Debrecen, Hungary, dios.szabolcs@eng.unideb.hu*
[2] *Debrecen University, Vehicles Engineering Department, Debrecen, Hungary, masuk@eng.unideb.hu*
[3] *Debrecen University, Faculty of Engineering, Debrecen, Hungary, tamasdinya@gmail.com*
[4] *Debrecen University, Doctoral School of Informatics, Debrecen, Hungary, szanto.attila@eng.unideb.hu*
[5] *Debrecen University, Mechanical Department, Debrecen, pettendid4@gmail.com*
[6] *Debrecen University, Mechatronics Department, Debrecen, balajti.istvan@eng.unideb.hu*

Abstract

The primary objectives of the project are to build a complex antenna rotation facility that will enable the structure to perform in situ interferometric measurements. The objectives include the construction of a stable frame to support and protect the control electronics, the design and fabrication of a 2.4GHz DTMPA (Dual Triangular Microstrip Patch antenna), and the support of the control electronics with the appropriate software background. The finished structure is capable of tracking the orbit of a satellite of your choice, up to NAP orbit depending on the configuration. The implementation can be divided into four steps. First of all, a sufficiently solid frame was designed and built. From the point of view of the use of materials, LEGO construction toys are the right choice, both in terms of weight and strength. The second step is to design and build the DTMPA. This is followed by the selection and implementation of the appropriate control electronics. The stepper motor must have adequate torque to ensure proper rotational motion, and the motor and microcontroller must provide clear instructions to the motors. Finally, the code responsible for controlling the motors must be written and implemented in the microcontroller so that the structure can be controlled by the appropriate external computer.

Keywords*: Interferometry, DTMPA, Antenna performance measurement, Microcontroller.*

1. Introduction

At the Faculty of Engineering, developments in the field of vehicles will be crucial in the coming years and research in this direction has been carried out at the Faculty [1–3]. There have also been advances in the field of artificial intelligence [4, 5]. The design provided by Cyber-Physical Systems has helped other research to progress faster [6, 7]. Taking this into account, the following paper has been prepared on the topic of radar sensors for vehicles.

In order to achieve the objectives set out, complex filming equipment will be designed and manufactured, as well as the DTMPA, which is essential for operation. A number of measurements necessary for antenna performance are carried out, which are essential for the completion of the task. After the integration of the software and hardware elements responsible for the movement, as well as the assembly of the finished system and the implementation of the software that serves them, the equipment can track the movement of a pre-selected satellite or the sun.

2. Radar Systems Need

This project introduces the concept of mechatronics, which has been used as a concept since the 1960s. This discipline combines mechanics, electronics, and computer technology, making it possible to create complex systems such as robots, engines, and electric vehicles [8, 9]. The topic is based on interferometric In Situ measure-

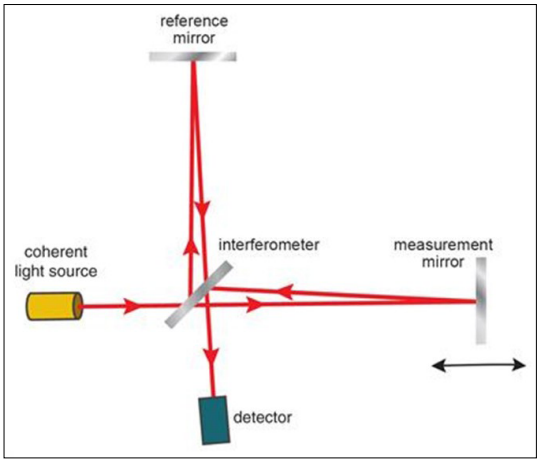

Fig. 1. *Basic principle of interferometry* **[11]**

ments. Interferometry is based on the principle of using waves, in a narrower circle, electromagnetic waves and then extracting information based on the phenomenon of interference created by them. Interferometry (**Fig. 1**) is a technique used to perform tasks that require very high measurement accuracy to measure the properties of various waves, vibrations, sounds, electromagnetism, or gravity. The most common fields of application for interferometry are astronomy, quantum physics, meteorology, and oceanography **[10]**. In industry, it is mainly used when measuring small displacements and unevenness.

3. Reqirement & Consideration

In order to achieve the objectives of the project, several coordinated areas must be created. A frame with a sufficiently stable base that holds the components together and provides them with mechanical protection is essential. It is essential to design and build a DTMPA with appropriate characteristics, as well as a stepper motor that ensures the rotation of this antenna, and the corresponding control electronics and software background.

Designing a DTMPA must be preceded by adequate research. An antenna is a transducer that transforms electromagnetic waves into electrical power and vice versa. It has the ability to operate as a transmitting and receiving antenna. In 1888, German physicist Heinrich Hertz constructed the first antennas **[12]**. James Clerk Maxwell's electromagnetic theory was confirmed through his experiments **[13]**.

The key invention for manipulating the components of the electromagnetic field, such as (1), (2), (3) and (4) is crucial in revealing the exponential function of the antenna's far-field pattern **[14]**.

$$E(r,\theta,\varphi)=E_1(r_1,\theta,\varphi)+E_2(r_2,\theta,\varphi)+E_3(r_3,\theta,\varphi)+E_4(r_4,\theta,\varphi) \quad (1)$$

In the far-field, the equation for the normalized scalar field is:

$$E(r,\theta,\phi) = f(\theta,\phi)\frac{e^{-jkr_1}}{r_1} - f(\theta,\phi)\frac{e^{-jkr_2}}{r_2} + + f(\theta,\phi)\frac{e^{-jkr_3}}{r_3} - f(\theta,\phi)\frac{e^{-jkr_4}}{r_4} \quad (2)$$

$$E(r,\theta,\phi)= \left[e^{+jkcos\psi_1} - e^{+jkcos\psi_2} + e^{+jkcos\psi_3} - e^{+jkcos\psi_4}\right] f(\theta,\phi)\frac{e^{-jkr}}{r} \quad (3),$$

where

$$\frac{E}{E_0} = AF(\theta,\phi) = 2[\cos(ks\ sin\theta cos\phi) - \cos(ks\ sin\theta\ sin\phi)] \quad (4)$$

The azimuth panel ($\theta = \pi/2$), along with the array factor of the entire reflector system reduce to:

$$\frac{E}{E_0} = AF\left(\theta = \frac{\pi}{2},\phi\right) = = 2[\cos(ks\ sin\theta cos\phi) - \cos(ks\ sin\theta\ sin\phi)] \quad (5)$$

The term "gain" refers to a parameter that indicates how ostensibly directed the radiation pattern of an antenna is. A low-gain antenna will radiate over a wide area, whereas a high-gain antenna will direct the majority of its power in a particular direction when it emits electromagnetic waves. At a wavenumber of zero ($k = 0$) and an azimuth angle ($\theta = 90°$), °), the antennas' phased array has a normalized power gain (G):

$$G\ (\theta) = \left|\frac{\sin\left(\frac{Nkd}{2}\right)\cos\theta}{N\sin\left(\frac{kd}{2}\right)\cos\theta}\right|^2 \quad (6)$$

A high-gain antenna has a longer range and better signal quality, but it must be developed, maintained, and installed in accordance with different antenna systems (**Fig. 2**).

After choosing the right antenna, it is necessary to determine the appropriate feeding method for the project objectives. The most common types of MPA antennas, due to their technical parameters and production costs, are the "monopole", "dipole" and "loop" antennas **[16]**.

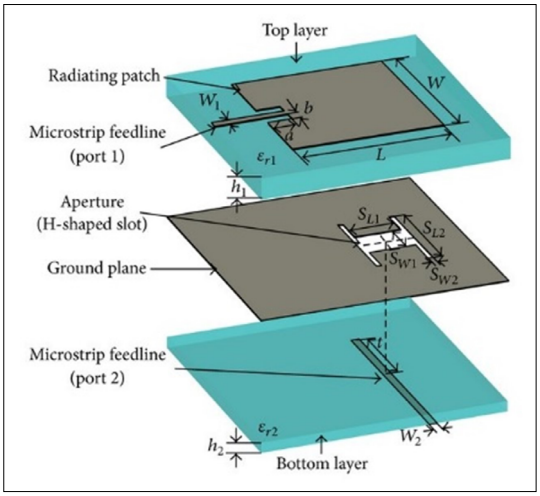

Fig. 2. *The microstrip patch antenna.* **[15]**

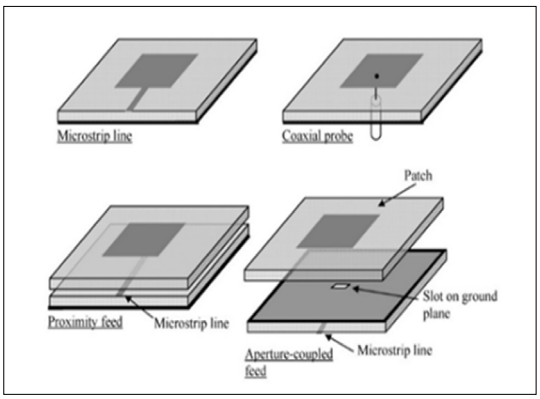

Fig. 3. *MPA feeding methods.*

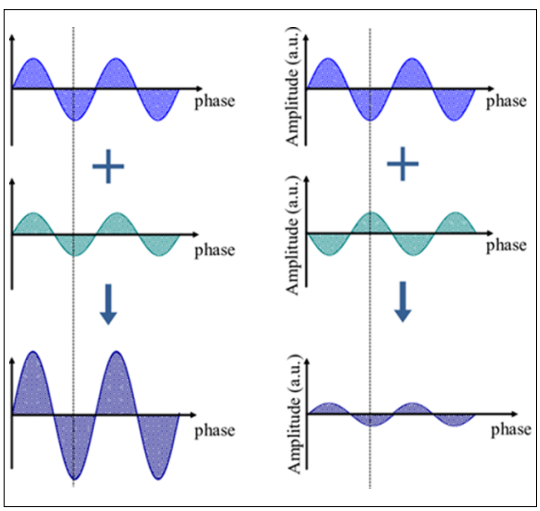

Fig. 4. *Constructive and destructive interference.*

These antennas must be powered in different ways. The four most common of these feeding methods are "microstrip line", "coaxial probe", "proximity feed" and "aperture-coupled feed". (**Fig. 3**).

In short, "microstrip feed" is the fastest and simplest, "aperture coupling" is the most difficult to manufacture, and "proximity coupling" has the highest bandwidth.

In the course of the literature review, the phenomenon of interference must be familiarized. We can talk about the phenomenon of interference interfering with measurements when the signal received in the bandwidth given by the antenna is mixed with other interfering signals, e.g. influenced or distorted by noise, modulated or other sources of electromagnetic radiation **[17]**. Interference can occur in several ways. It can be caused by nearby antennas, metal objects interacting with each other, or the presence of electronic devices. At the same time, naturally occurring lightning and other nearby buildings and rock walls can also cause reflections. A common cause of interference is the presence and proximity of other antennas operating in the same frequency range. Signals reflected back from different signal sources or from objects in our environment interfere with each other as described in Chapter 1. . Consequently, the signal strength we expect is reduced, distorted, and the signal-to-noise interference ratio can lead to complete signal loss. It can often be caused by electronic devices, such as radio-television transmission towers, electronic wires, or other communication equipment and other electronic noise sources (**Fig. 4**).

In order to move the corresponding components, it is necessary to embed stepper motors **[18]**. This type of motor is a brushless design, otherwise known as BLDC (brushless DC), which causes the rotating movement with a series of electrical pulses. In terms of operation, they can be divided into two parts, a stationary (stator) and a rotating (rotor) par **[19]**. In terms of design, it can be permanent magnetic, where the rotating part is a permanent magnet, as well as variable reluctance, where the rotating part is a plated iron core, which is magnetized by an electric current. The hybrid engine is a combination of these two designs **[20, 21]**. Their operating principle is based on magnetic attraction. Both the stationary and the rotating parts have teeth and grooves on which, if an opposite magnetic polarity develops, the half of the tooth with the opposite polarity closest to it in space moves, if the distance be-

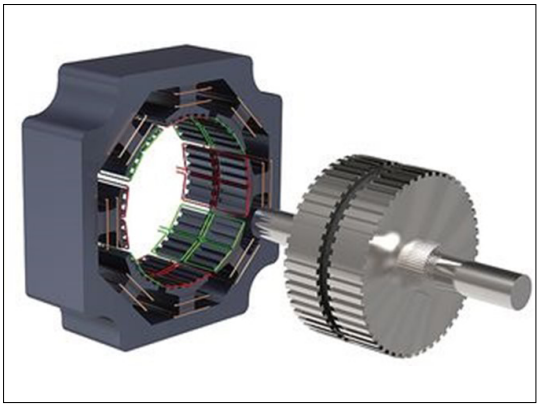

Fig. 5. *Hybrid stepping motor* [22]

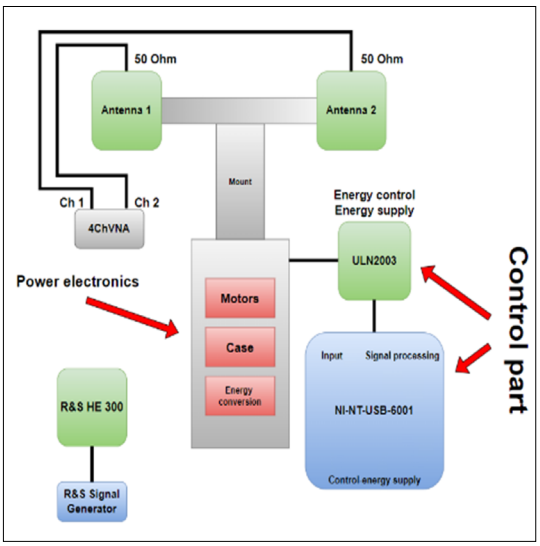

Fig. 6. *The antenna mast and the subsystems required for operation*

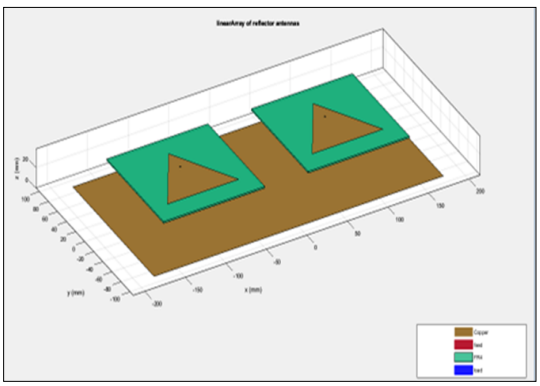

Fig.7. *Dual Triangular Microstrip Patch antenna (DTMPA)*

tween them is sufficiently small. We call this a surprise , hence the term stepper motor. This step can be full, up or micro surprise. In the case of a hybrid stepper motor (Fig. 5) the rotating part is the shaft itself, with two reluctance type ferromagnets with a phase shift of half from each other, and a permanent magnet with axial magnetization between them. The rotating part segments represent opposite magnetic poles.

4. Findings

The assembly of the finished, working equipment of the project was preceded by thorough research work. Fig.6 illustrates the structure of the equipment.

The signals received by the antennas controlled by the antenna mast are sent to the 4ChVNA device, amplitude and phase are correctly sampled and then processed. The task of the R&S signal generator in actuator mode is to generate the desired signal structures and sequences and transmit them to the antennas via a 50 Ohm cable.

4.1. The DTMPA Antenna

An important aspect of the project is the DTMPA located on top of the camera. The construction of this antenna was preceded by several design processes. The most important of these is designing the antenna in the MATLAB simulation environment. During the design process, with the help of the "antenna array designer" built into the software, and by specifying the desired 2.4GHz frequency, the software simulated the rough sketch of the future antenna. This sketch (Fig. 7) required many manual corrections in order to function properly. (e.g. material use, substrate thickness).

4.2. The antenna mast and the subsystems required for operation

The construction of the DTMPA presented above has always been among the objectives. Once the design process is completed, the achieved results will be produced at a later date due to financial reasons, with the recognition of the expert opinion of the faculty. The rationale for this was keeping costs and time efficiency in mind. In addition, it is important to point out that the department had several existing antennas at the end of the design, several of which met the objectives of the project. Therefore, in the future, we will use two existing antennas in order to achieve the goal, the documentation and measurement results of which are detailed below.

The physical parameters of the provided antennas are the same. Both use an FR4 substrate, on which the "slot" itself is located. This is followed by an air substrate layer, and then a copper base plate is placed below this. The distance between the two plates, i.e. the λ/4 value for both antennas, is 5.4 cm. The double of this, i.e. the λ/2 value, will be the distance that must be between the feed points of the two antennas in order to be used in an "array" design. Both antennas receive power through a standard coaxial connector located at the bottom of the antenna. Fig. 8. and 9 show some measured values of the "L" band antenna and Table 1. shows "L" band antenna performance measurements with different frequencies.

Table 1. *„L" band antenna performance measurements with different frequencies*

„L" band antenna		
Frequency	**1.3 GHz**	**2.4 GHz**
Back radiation	-46.6dB	-43.6dB
Turned 60˚to the right from the main beam	-39.5dB	-37.5dB
Turned 60˚to the left from the main beam	-37.6dB	-36.2dB
Main beam maximum (horizontal polarization)	-25.6dB	-24.6dB
Cross polarization value	-58.6dB	-58.2dB
Main beam maximum (vertical polarization)	-25.8dB	-22.6dB

5. Antenna Performance Measurement

The antenna used in the project had to be subjected to measurements in order to gain certainty that it is suitable for the objectives of the topic. For this purpose, two measurements were performed. A simple antenna performance measurement, as well as a more complex near-field antenna measurement. We determined the characteristics of the existing slot resonator antenna with two independent measurements. The first measurement was taken from several different positions in the case of a fixed antenna. In the assembly according to Fig. 10. Several different measuring devices were used for the measurement. The ROHDE & SCHWARZ SMB 100B signal generator supplying the antenna provided the necessary signals, first at 1.3 and then at 2.4 GHz frequency. For both settings, a "level" value of 4dBm was set.

During the measurement shown in Fig. 11 we used a 360-degree rotatable measuring bench in order to determine the 360-degree characteristic of the antenna. We used an R&S HE 300 antenna connected to a 4ChVNA signal generator as a "transmitting" antenna. The data was evaluated on a computer connected to the signal generator. The distance between the "receiver" and "transmitter" antenna was 2.6m. During the measurement, we slowly turned the rotatable measuring bench around several times, and then performed the same sequence of movements in the opposite direction. Fig. 12 shows the rotatable measuring bench.

5.1. Stepper Motor Subsystem

The frame is moved by two mini stepping motors. In terms of their movement, horizontal and vertical circular movement. The lower motor ensures the rotation of the frame on the axis, while

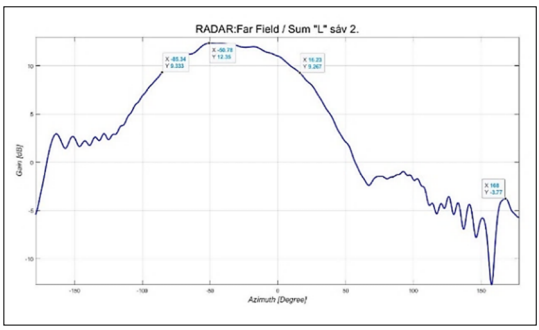

Fig. 8. *Measured "L" band antenna radiation pattern.*

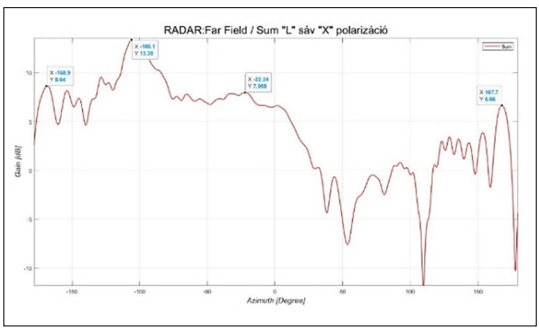

Fig. 9. *Measured "L" band antenna radiation pattern with x-polarization.*

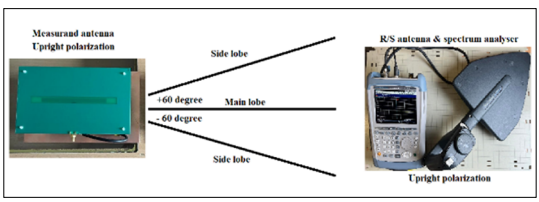

Fig.10. *Simplified antenna characteristic measurement arrangement*

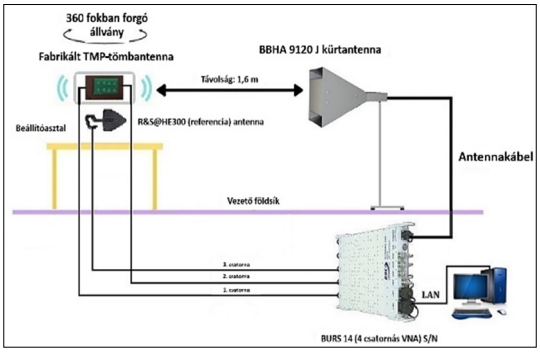

Fig. 11. *Description of the measurement environment.*

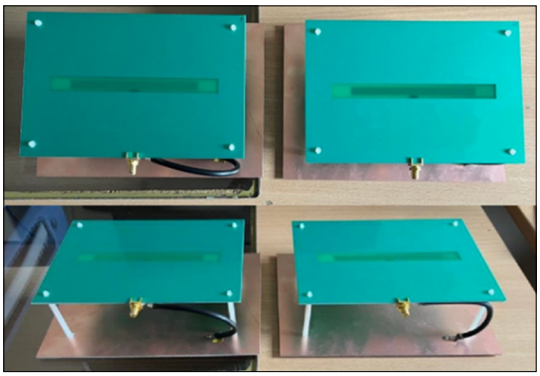

Fig. 12. *„L" band antennas.*

```
azMaxStep = 100
elMaxStep = 100
azMax = 360
elMax = 90


NoHaltMotorsGlobal = True
donePositioning = True
resetMotors = False
calibration = False
doneCalibration = False
currAzPos = 0
currElPos = 0
shutdownThreads = False
```

Fig. 13. *The maximum number of steps for running the motors.*

```
def set_output_states(states,stepDelay,sel):
    if sel==1:
        for i in range(len(states)):
            task2.write(np.array(states[i], dtype=bool), auto_start=True)
            if stepDelay != 0:
                time.sleep(stepDelay)
    else:
        for i in range(len(states)):
            task1.write(np.array(states[i], dtype=bool), auto_start=True)
            if stepDelay != 0:
                time.sleep(stepDelay)
    return 0
```

Fig. 14. *The code responsible for the function causes the motors to move.*

the upper one rotates the antenna support panel vertically at the desired angle. **Fig. 13** shows the maximum number of steps for the specified position angle and lateral angle, as well as the declared variables that the main thread writes to instruct the thread responsible for running the motors.

The two SM-28BYJ-48-5V motors used **[23]** are four-phase, unipolar. Its torque is adequate, taking into account the above-mentioned weight issue, so it is able to ensure the appropriate rotational movement. The motor located at the top of the structure is directly responsible for the vertical rotation of the antenna, while the lower one is responsible for the horizontal rotation of the entire frame. **Fig. 14** shows the code fragment responsible for the function that causes the motors to move clockwise and counterclockwise.

The motor can be controlled with two motor controllers, nominally a ULN2003. Its physical appearance can be seen in **Fig. 15**.

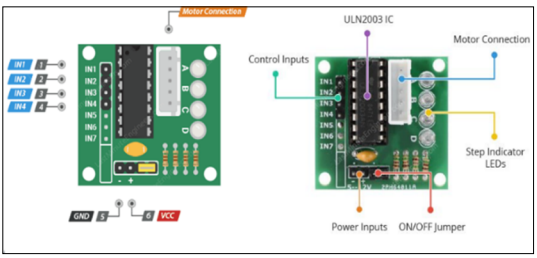

Fig. 15. *ULN2003 motor controller.*

5.2. Stepper Motor Programming

The project uses a NI USB 6001 data acquisition card connected to a computer that supplied it with the control commands. An application written in the Python programming language is running on this computer. The NI DAQMX library was imported into the mentioned Python code, which contains the functions needed to control the data acquisition card. The communication protocol

used by the hamLib library in the TCP/IP application layer was implemented in the same code.

The gpredict open-source software was chosen as the basis for the engine control.

Gpredict is a real-time satellite tracking and prediction app. It monitors and displays satellite positions and data through lists, tables, maps, and polar plots. It forecasts future satellite passes, and uniquely, you can group satellites into customizable modules for a personalized look and functionality. Plus, Gpredict can track satellites from multiple observer locations concurrently, but its key advantage is that it can handle antenna rotators and radios that support the hamlib protocol.

So gpredict tracks the selected satellite, calculates the azimuth and elevation angles for the rotator according to our own position and transmits via TCP/IP using hamlib protocol at the application layer.

A program written in Python receives commands as a server through the hamlib protocol and controls and monitors the stepping motors via a NI USB 6001 device. In the first step, the program initializes and loads the appropriate libraries to control the NI USB 6001, then loads the configuration file, which specifies how many steps it can take on each of the two axes, and in the final states, the angles at which the steps correspond according to the hamlib.

In calibration mode, the axes can be moved independently; if you reach the end stop on one axis, the counter will be reset; if you move it in the opposite direction, the counter will count each step instruction.

If we think we have reached the maximum possible step on a given axis or the limit stop is pressed again, we can save the maximum possible steps in a configuration file.

In normal running mode, after loading the configuration file, a TCP/IP server is started, which decodes the hamlib commands and gets the positions in angles. These angles are converted into step numbers according to the configuration file. From then on, the control works like a CNC machine; the program knows exactly how many steps the motor is taking in relation to the end position, "governs" it so that the set steps are not exceeded, and knows how many steps to take in one direction or the other in relation to the new position. Fig. 16 shows the software topology.

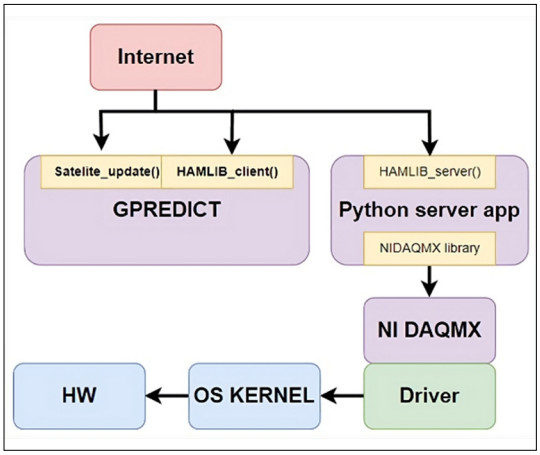

Fig. 16. *Software topology.*

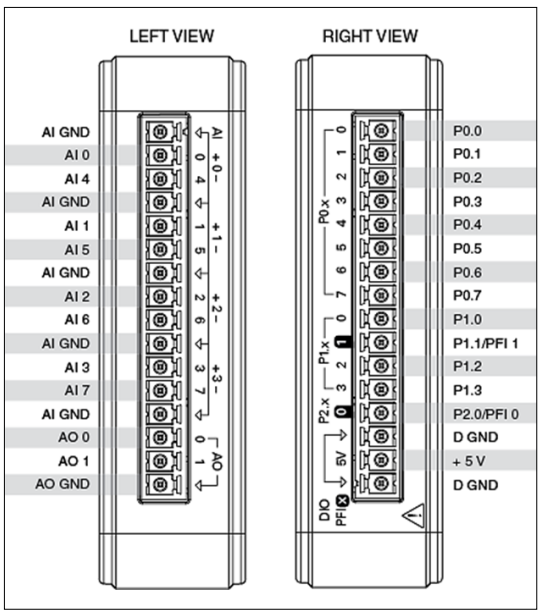

Fig. 17. *NI-NT-USB-6001.*

5.3. Software topology

The stepper motors are controlled by a microcontroller that schedules and supplies the motors with the appropriate instructions. The choice fell on a NI-NT-USB-6001 device. See in Fig. 17, the NI-NT-USB-6001 is a versatile device suitable for many applications including laboratory experiments, research and development, and industrial automation. Due to its small size, portability and easy handling, it offers an ideal solution for many measurement and control tasks, such as for moving the antenna system of the interferometer stand. The NI-NT-USB-6001 is a multifunction data acquisition device designed and manufactured by National Instruments (NI). The device is a small,

portable USB-based data acquisition module that provides analog and digital inputs and outputs, as well as a counter/timer function. NI-NT-USB-6001 has 8 analog input channels with 14-bit resolution and 48 kS/s sampling rate. It has 2 analog output channels with 16-bit resolution and a maximum update rate of 2 kS/s [24].

5.4. The Build Area Unit

To hold the various electronic components together, as well as to fix the antenna, a frame is required that is sufficiently stable. In order for the appropriate elements to be fixed, a complex framework had to be created that meets several aspects. First of all, it was necessary to take care of the understanding of the two stepping motors, since thanks to them the rotating movement is realized. In addition, proper fixing of the microcontroller and the mounting panel is also crucial. One of the most critical features of a frame is its weight. Stepper motors have a maximum load capacity. Exceeding this, the system will not be able to function properly as far as the rotary movement is concerned. Although the metal house is the most durable and stable, due to the weight limit, we decided on the plastic building equipment called LEGO. Sufficiently stable, highly customizable.

However, it is important to note that LEGO is made from ABS, an industrial plastic. Before building the Antenna frame, 3D modelling [26] was carried out. This will make it easier to redesign and to see the frame to be built in a virtual framework. We can also make the necessary parts list. The free BrickLink studio [26] was used for modelling, allowing the design of customized components, import and export of models and the creation of building guides.

Once the design was complete, a list of the elements needed to build it was available. Minimal modification was required to the physical antenna rotator (see Fig. 19).

After building and testing the project, it can be determined that it meets the expected and defined requirements. The motors are able to rotate the frame adequately, the Python application properly handles and transmits the signals, and the measured characteristics of the antenna are also suitable for the objectives.

6. Conclusions

In the course of the project, opportunities for further development arose in several directions. Perhaps the most important of these is the design of

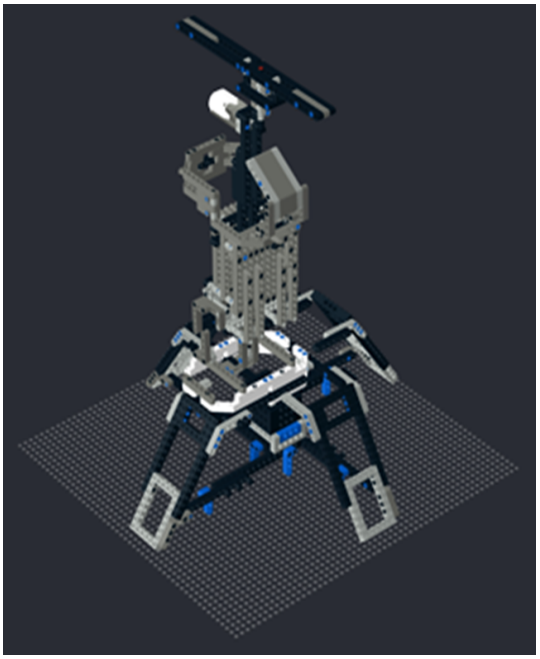

Fig. 18. *3D designed of the antenna frame.*

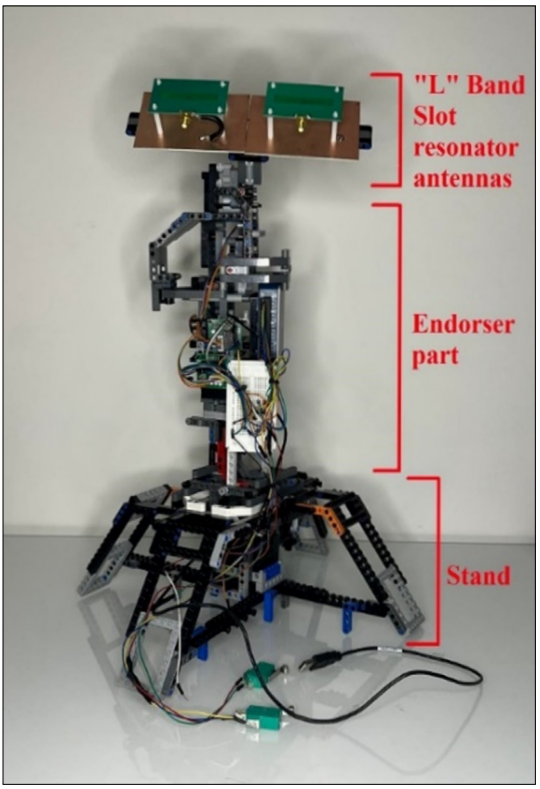

Fig. 19. *Designed and assembled antenna rotation system.*

an even more durable metal frame, but this significantly increases both the material and, more importantly, the weight factor affecting transportability.

The stepper motor has a specific torque that had to be kept in mind during construction. This problem can be eliminated with more powerful engines, but this also involves increased weight, so it is important to find the right balance. It should be mentioned that if an encoder is built into the system, even more precise motor positioning can be achieved.

A further development option in another direction is a completely waterproof outer covering, thanks to which the construction becomes capable of outdoor operation regardless of the weather. A further development option is a higher-gain, directional phase-controlled antenna system with a preamplifier, which enables more precise measurements.

This research could be of help, in vehicle topics that we have previously researched in the university such as lightweight aircraft and antenna design **[27, 28]**.

Acknowledgement

Special thanks for the support to the University of Debrecen, Faculty of Engineering.

References

[1] T. I. Erdei, Z. Molnár, N. C. Obinna, G. Husi: *A Novel Design of an Augmented Reality Based Navigation System &Amp; Its Industrial Applications.* ACTA IMEKO, 7/1. (2018) 57. https://doi.org/10.21014/acta_imeko.v7i1.528

[2] T. I. Erdei, N. C. Obinna, Z. Molnar, G. Husi: *Surveillance and Security System in the Building Mechatronics Research Center*. In: 2017 International Conference on Engineering, Technology and Innovation (ICE/ITMC), IEEE, Jun. 2017. 509–512. https://doi.org/10.1109/ICE.2017.8279928

[3] T. I. Erdei, Z. Molnár, G. Husi: *Selecting Equipment and Supplies for Self–Replicating 3D Printer*. ACTA Tech. CORVINIENSIS - Bull. Eng., 2016, [Online]. Available: https://www.researchgate.net/publication/296696614_Selecting_Equipment_and_Supplies_for_Self-Replicating_3D_Printer

[4] T. P. Kapusi, T. I. Erdei, G. Husi, A. Hajdu: *Application of Deep Learning in the Deployment of an Industrial SCARA Machine for Real-Time Object Detection*. Robotics, 11/4. (2022) 69. https://doi.org/10.3390/robotics11040069

[5] T. I. Erdei, G. Husi: *Singularity Measurement in the Cyber-Physical and Intelligent Robot Systems Laboratory*. Int. Rev. Appl. Sci. Eng., 11/2. (2020) 82–87. https://doi.org/10.1556/1848.2020.20001

[6] T. I. Erdei, R. Krakó, G. Husi: *Design of a Digital Twin Training Centre for an Industrial Robot Arm*. Appl. Sci., 12/17. (2022) 8862. https://doi.org/10.3390/app12178862

[7] A. Masuk, I. Balajti: *Mechatronics Engineering Aspects of VHF Band Antenna Design of Industry 4.0 Applications*. In: 23rd International Radar Symposium (IRS), IEEE, Sep. 2022, 77–82. https://doi.org/10.23919/IRS54158.2022.9905051

[8] D. A. Bradley, N. C. Burd, D. Dawson, A. J. Loader: *Mechatronics Electronics in Products and Processes*. 1st ed. London, Routledge, 2018. https://doi.org/10.1201/9780203747735

[9] U. S. Dixit, M. Hazarika, J. P. Davim: *History of Mechatronics.* In: *A Brief History of Mechanical Engineering*. Springer, 2017. 147–164. https://doi.org/10.1007/978-3-319-42916-8_7

[10] P. Hariharan, K. Creath: *Basics of Interferometry*. Phys. Today, 46/1. (1993) 75–75. https://doi.org/10.1063/1.2808787.

[11] "How Do Interferometric Systems Work," Renishaw. [Online]. Available: https://www.renishaw.com/en/how-do-interferometric-systems-work--38612

[12] M. M. Wang, J. Zhang: *Machine-Type Communication for Maritime Internet-of-Things*. Springer International Publishing, 2021. https://doi.org/10.1007/978-3-030-77908-5

[13] D. L. Sengupta, T. K. Sarkar: *Maxwell, Hertz, the Maxwellians, and the Early History of Electromagnetic Waves*. IEEE Antennas Propag. Mag., 45/2. (2003) 13–19. https://doi.org/10.1109/MAP.2003.1203114.

[14] B. A. Kemp: *Resolution of the Abraham-Minkowski Debate: Implications for the Electromagnetic Wave Theory of Light in Matter*. J. Appl. Phys., 109/11. (2011) 111101. https://doi.org/10.1063/1.3582151

[15] Y. Liu, H. Yang, S. Mao, J. Zhu: *A Multibeam Dual-Band Orthogonal Linearly Polarized Antenna Array for Satellite Communication on the Move*. Int. J. Antennas Propag., 2015. 1–8. https://doi.org/10.1155/2015/102959.

[16] D. F. Sievenpiper et al.: *Experimental Validation of Performance Limits and Design Guidelines for Small Antennas.* IEEE Trans. Antennas Propag., 60/1. (2012) 8–19. https://doi.org/10.1109/TAP.2011.2167938.

[17] N. I. Miridakis, D. D. Vergados: *A Survey on the Successive Interference Cancellation Performance for Single-Antenna and Multiple-Antenna OFDM Systems*. IEEE Commun. Surv. Tutorials, 15/1. (2013) 312–335. https://doi.org/10.1109/SURV.2012.030512.00103.

[18] A. Szántó, S. Hajdu, G. Á. Sziki: *Dynamic Simulation of a Prototype Race Car Driven by Series Wound DC Motor in Matlab- Simulink*. Acta Polytechnica Hungarica, 17/4. (2020) 103–122. https://doi.org/10.12700/APH.17.4.2020.4.6.

[19] C. Pollock, J. D. Wale: *Hybrid Stepping Motors and Drives*," Power Eng. J., 5/1. (2001). 5–12. https://doi.org/10.1049/pe:20010101.

[20] G. Á. Sziki, A. Szántó, J. Kiss, G. Juhász, É. Ádámkó: *Measurement System for the Experimental Study and Testing of Electric Motors at the Faculty of Engineering, University of Debrecen.* Appl. Sci., 12/19. (2022) 10095. https://doi.org/10.3390/app121910095.

[21] A. Szántó, É. Ádámkó, G. Juhász, G. Á. Sziki: *Simultaneous measurement of the Moment of Inertia and Braking Torque of Electric Motors Applying Additional Inertia.* Measurement, 204. (2022) 112135. https://doi.org/10.1016/j.measurement.2022.112135

[22] I. Don Labriola P.E. President, QuickSilver Controls, "The Hybrid Servomotor: Stepping up to Closed Loop," Motion Control Tips. [Online]. https://www.motioncontroltips.com/the-hybrid-servomotor-stepping-up-to-closed-loop/

[23] "28BYJ-48-64 64:1 Stepper Gearmotor," Solarbotics. [Online]. https://www.solarbotics.com/product/22310/

[24] "NI USB-6002 Low-Cost DAQ USB Device," NI. [Online]. https://www.ni.com/docs/en-US/bundle/usb-6002-specs/resource/374371a.pdf

[25] T. Istvan Erdei, R. Krako, N. David Peter, G. Husi: *3D CAD Design of KUKA Robot Arm &Amp; Integration into AR Environment to Educational Purposes*. In: IEEE 20th International Power Electronics and Motion Control Conference (PEMC), IEEE, Sep. 2022, 590–596. https://doi.org/10.1109/PEMC51159.2022.9962864

[26] "LEGO® Digital Designer," BrickLink Studio. [Online]. Available: https://www.bricklink.com/v3/studio/download.page

[27] A. Masuk, H. Géza: *Aero Graphene in Modern Aircraft & UAV.* Recent Innovations in Mechatronics, 9/1. (2022). https://doi.org/10.17667/riim.2022.1/4.

[28] A. Masuk, H. Géza: *Uses of Aero Graphene and CNT in Modern Aircraft*. AIP Conference Proceedings, 2941/1. (2023) 020029. https://doi.org/10.1063/5.0181354.